


Research Article

Optical Solitons with Dispersive Concatenation Model Having Fractional Temporal Evolution

Ahmed H. Arnous¹, Muhammad Amin S. Murad², Anjan Biswas^{3,4,5,6} , Yakup Yildirim^{7,8*}, Luminita Moraru^{9,10}

¹Department of Engineering Mathematics and Physics, Higher Institute of Engineering, El-Shorouk Academy, Cairo, Egypt

²Department of Mathematics, College of Science, University of Duhok, Duhok, Iraq

³Department of Mathematics and Physics, Grambling State University, Grambling, LA, 71245-2715, USA

⁴Department of Physics and Electronics, Khazar University, Baku, AZ, 1096, Azerbaijan

⁵Department of Applied Sciences, Cross-Border Faculty of Humanities, Economics and Engineering, Dunarea de Jos University of Galati, 111 Domneasca Street, Galati, 800201, Romania

⁶Department of Mathematics and Applied Mathematics, Sefako Makgatho Health Sciences University, Medunsa, 0204, South Africa

⁷Department of Computer Engineering, Biruni University, Istanbul, 34010, Turkey

⁸Mathematics Research Center, Near East University, 99138, Nicosia, Cyprus

⁹Department of Chemistry, Physics and Environment, Faculty of Sciences and Environment, Dunarea de Jos University of Galati, 47 Domneasca Street, 800008, Romania

¹⁰Department of Physics, School of Science and Technology, Sefako Makgatho Health Sciences University, Medunsa, 0204, Pretoria, South Africa

E-mail: yyildirim@biruni.edu.tr

Received: 3 January 2025; **Revised:** 14 March 2025; **Accepted:** 31 March 2025

Abstract: This paper adopts the direct algebraic method to recover and enlist a full spectrum of optical 1-soliton solutions for the dispersive concatenation model that comes with Kerr law of nonlinear refractive index change. The temporal evolution for the model is taken to be fractional so that the model is viable for controlling the Internet bottleneck-a growing problem in telecommunications industry. The numerical simulations supplement the soliton solutions that are obtained analytically.

Keywords: solitons, Kerr, fractional

MSC: 78A60

1. Introduction

The year was 2014. It was exactly a decade ago when a very interesting model that describes the propagation of optical solitons was conceived. This is the concatenation model [1, 2]. It is formed by combining the nonlinear Schrödinger's equation (NLSE) [3–5], Lakshmanan-Porsezian-Daniel (LPD) model [6–8] and the Sasa-Satsuma equation [9, 10]. This model was extensively studied from a wide range of angles that includes the Painleve analysis, identifying a full spectrum of 1-soliton solutions, bifurcation analysis, locating the conservation laws, recovering the gap solitons in Bragg gratings as well as checking out the implicit quiescent optical solitons with nonlinear chromatic dispersion (CD) and many others.

Copyright ©2025 Yakup Yildirim, et al.

DOI: <https://doi.org/10.37256/cm.6220256344>

This is an open-access article distributed under a CC BY license

(Creative Commons Attribution 4.0 International License)

<https://creativecommons.org/licenses/by/4.0/>

Subsequently, later during the same year, as well as in 2015, a new form of this concatenation model came into existence, proposed by the same group from Australia. This is being referred to as the dispersive concatenation model. This is formulated with the conjunction of the Schrödinger-Hirota equation (SHE), LPD and the fifth-order NLSE. Two of the components from this model, namely SHE and the fifth-order NLSE contribute to the dispersive effects of the solitons for this model and hence the name dispersive concatenation model. Later this model too was extensively addressed from the same wide range of perspectives, namely the conservation laws, bifurcation analysis, quiescent optical solitons for nonlinear CD and other such aspects.

Subsequently, both of the models were addressed with power-law of self-phase modulation (SPM) where many such features are illustrated. Lately, both of these models were considered with differential group delay and the relevant results were also recovered [11–14]. It is now time to bridge the gap by addressing the models with fractional temporal evolution. The concatenation model was already addressed from this point of view [6]. The current paper details the study of the dispersive concatenation model with fractional temporal evolutions as a follow-up of the previous paper. The adopted integration scheme is the enhanced direct algebraic method that yield a plethora of results including the full spectrum of optical solitons. These solitons are obtained through the intermediary Jacobi's elliptic functions that gave way to the soliton solutions when the modulus of ellipticity approached a specific limiting value. The details of the mathematical analysis are exhibited in the rest of the paper and the analytical results are also supplemented with captivating numerical simulations.

1.1 Governing model

The following formulation presents the dimensionless concatenation model that captures soliton propagation through optical fibers with fractional temporal evolution [11–14]:

$$\begin{aligned}
 & i \frac{\partial^\alpha q}{\partial t^\alpha} + a q_{xx} + b |q|^2 q - i c_1 \left(\delta_1 q_{xxx} + \delta_2 |q|^2 q_x \right) \\
 & + c_2 \left(\delta_3 q_{xxxx} + \delta_4 |q|^2 q_{xx} + \delta_5 |q|^4 q + \delta_6 |q_x|^2 q + \delta_7 q_x^2 q^* + \delta_8 q_{xx}^* q^2 \right) \\
 & - i c_3 \left(\delta_9 q_{xxxxx} + \delta_{10} |q|^2 q_{xxx} + \delta_{11} |q|^4 q_x + \delta_{12} q q_x q_{xx}^* + \delta_{13} q^* q_x q_{xx} + \delta_{14} q q_x^* q_{xx} + \delta_{15} q_x^2 q_x^* \right) = 0.
 \end{aligned} \tag{1}$$

Here, in Eq. (1), the wave amplitude is designated to be $q(x, t)$ and is a complex-valued function where $i = \sqrt{-1}$ while the variables x and t represent the spatial and temporal variables respectively. The coefficient of a is the linear chromatic dispersion while the coefficient of b is the self-phase modulation that comes from Kerr law of nonlinear refractive index change. The first three terms together with the coefficient of c_1 represents the SHE. Next, the coefficient of c_2 gives the LPD operator while the coefficient of c_3 accounts for the fifth-order NLSE. Thus, the model carries third-order, fourth-order and fifth-order dispersion terms. These therefore make it into a truly dispersive concatenation model. One of the salient features of a dispersive model is the soliton radiation. This would drastically slow down the soliton velocity. However, such effects are totally ignored and the focus on this paper would be on the core soliton region or on the discrete regime of the wave. The parameter α is the measure of the fractional temporal evolution where $0 < \alpha \leq 1$. The analysis of the model will now be carried out in the subsequent sections to retrieve optical solitons with fractional temporal evolution after a quick recapitulation of the fundamental concepts from fractional calculus.

The paper is structured as follows: Section 2 presents the mathematical preliminaries, outlining the fundamental equations, definitions, and theoretical background relevant to the study. Section 3 delves into the mathematical analysis, where the governing equations are examined, and essential properties such as existence conditions are discussed. In Section 4, the integration algorithm is introduced, detailing the analytical technique used to solve the problem, along with their implementation properties. Section 5 focuses on the application to the model, demonstrating how the developed

method is applied to a specific system, with parameter selection and case studies. Section 6 provides the results and discussion, presenting analytical findings, graphical representations, and a comprehensive analysis of the outcomes. Finally, Section 7 concludes the paper, summarizing key findings, highlighting the study's contributions, and suggesting directions for future research.

2. Mathematical preliminaries

A summary of the conformal fractional derivative from basic fractional calculus is addressed below, including the fundamental properties necessary for deriving the solutions to the model investigated in [6].

2.1 Introduction

Assuming $f : [0, \infty) \rightarrow \mathbb{R}$ and $0 < \alpha \leq 1$, the conformable fractional derivative of f of order α is characterized by [6]:

$$L_{\alpha}(f)(x) = \lim_{\varepsilon \rightarrow 0} \frac{f(x + \varepsilon x^{1-\alpha}) - f(x)}{\varepsilon}, \quad (2)$$

for all $x > 0$ and $\alpha \in (0, 1]$.

Let $0 < \alpha \leq 1$, $a, b, p \in \mathbb{R}$ and $f(x), g(x)$ be α -differentiable, at a point $x > 0$. Then

$$(1) L_{\alpha}(af(x) + bg(x)) = aL_{\alpha}f(x) + bL_{\alpha}g(x)$$

$$(2) L_{\alpha}(x^p) = px^{p-\alpha}$$

$$(3) L_{\alpha}(\mu) = 0, \quad \mu \text{ is constant}$$

$$(4) L_{\alpha}\left(\frac{f(x)}{g(x)}\right) = \frac{gL_{\alpha}(f(x)) - fL_{\alpha}(g(x))}{g(x)^2}$$

$$(5) \text{ If in addition } f \text{ is differentiable then}$$

$$L_{\alpha}f(x) = x^{1-\alpha} \frac{df(x)}{dx} \quad (3)$$

3. Mathematical analysis

The approach outlined below is employed to address Eq. (1):

$$q(x, t) = U(\eta)e^{i\varphi(x, t)}, \quad (4)$$

where

$$\eta = k\left(x - v\frac{t^{\alpha}}{\alpha}\right). \quad (5)$$

For this case, v represents the speed, η signifies the wave variable, $U(\eta)$ denotes the amplitude, and the phase component $\varphi(x, t)$ is expressed as:

$$\varphi(x, t) = -\kappa x + \omega \frac{t^\alpha}{\alpha} + \vartheta_0. \quad (6)$$

With ϑ_0 as the phase constant, ω as the wave number, and κ as the frequency, substitution of Eq. (4) into Eq. (1), followed by decomposition into real and imaginary components, results in:

$$\begin{aligned} & \left(a\kappa^2 + c_3\kappa^5\delta_9 - c_2\kappa^4\delta_3 - c_1\kappa^3\delta_1 + \omega \right) U(\eta) - k^2 \left(a + 10c_3\kappa^3\delta_9 - 6c_2\kappa^2\delta_3 - 3c_1\kappa\delta_1 \right) U''(\eta) \\ & + \left(-c_3\kappa^3\delta_{10} - c_3\kappa^3\delta_{12} - c_3\kappa^3\delta_{13} + c_3\kappa^3\delta_{14} + c_3\kappa^3\delta_{15} + c_2\kappa^2(\delta_4 - \delta_6 + \delta_7 + \delta_8) + c_1\kappa\delta_2 - b \right) U(\eta)^3 \\ & + k^2 \left(c_3\kappa(-2\delta_{12} + 2\delta_{13} + 2\delta_{14} + \delta_{15}) - c_2(\delta_6 + \delta_7) \right) U(\eta)U'(\eta)^2 + (c_3\kappa\delta_{11} - c_2\delta_5)U(\eta)^5 \\ & + k^2 \left(c_3\kappa(3\delta_{10} + \delta_{12} + \delta_{13} - \delta_{14}) - c_2(\delta_4 + \delta_8) \right) U(\eta)^2U''(\eta) + k^4(5c_3\kappa\delta_9 - c_2\delta_3)U^{(4)}(\eta) = 0, \end{aligned} \quad (7)$$

$$\begin{aligned} & k \left(2a\kappa + 5c_3\kappa^4\delta_9 - 4c_2\kappa^3\delta_3 - 3c_1\kappa^2\delta_1 + v \right) U'(\eta) + c_3k^3\delta_{15}U'(\eta)^3 + c_3k\delta_{11}U(\eta)^4U'(\eta) \\ & + k \left(\kappa(c_3\kappa(-3\delta_{10} + \delta_{12} - 3\delta_{13} + \delta_{14} + \delta_{15}) + 2c_2(\delta_4 + \delta_7 - \delta_8)) + c_1\delta_2 \right) U(\eta)^2U'(\eta) \\ & + k^3(2\kappa(2c_2\delta_3 - 5c_3\kappa\delta_9) + c_1\delta_1)U^{(3)}(\eta) + c_3k^3(\delta_{12} + \delta_{13} + \delta_{14})U(\eta)U'(\eta)U''(\eta) \\ & + c_3k^3\delta_{10}U(\eta)^2U^{(3)}(\eta) + c_3k^5\delta_9U^{(4)'}(\eta) = 0. \end{aligned} \quad (8)$$

The velocity is derived from the imaginary part:

$$v = -2a\kappa + 4c_2\kappa^3\delta_3 + 3c_1\kappa^2\delta_1, \quad (9)$$

and

$$\kappa(2c_2\chi - 4c_3\kappa\delta_{13}) + c_1\delta_2 = 0, \quad (10)$$

with $\chi = \delta_4 + \delta_7 - \delta_8$. The frequency is described by Eq. (8), along with constraint relations:

$$\delta_9 = \delta_{10} = \delta_{11} = \delta_{15} = 0, \quad (11)$$

$$\delta_{12} + \delta_{13} + \delta_{14} = 0, \quad (12)$$

$$4c_2\kappa\delta_3 + c_1\delta_1 = 0. \quad (13)$$

Then Eq. (1) reduces to

$$\begin{aligned}
 & i q_t + a q_{xx} + b |q|^2 q - i c_1 \left(\delta_1 q_{xxx} + \delta_2 |q|^2 q_x \right) \\
 & + c_2 \left(\delta_3 q_{xxxx} + \delta_4 |q|^2 q_{xx} + \delta_5 |q|^4 q + \delta_6 |q_x|^2 q + \delta_7 q_x^2 q^* + \delta_8 q_{xx}^* q^2 \right) \\
 & - i c_3 \left(\delta_{12} q q_x q_{xx}^* + \delta_{13} q^* q_x q_{xx} + \delta_{14} q q_x^* q_{xx} \right) = 0,
 \end{aligned} \tag{14}$$

and Eq. (7) reaches

$$\begin{aligned}
 & (a \kappa^2 + \kappa^3 (- (c_2 \kappa \delta_3 + c_1 \delta_1)) + \omega) U(\eta) + (2 c_3 \kappa^3 \delta_{14} + c_2 \kappa^2 (\delta_4 - \delta_6 + \delta_7 + \delta_8) + c_1 \kappa \delta_2 - b) U(\eta)^3 \\
 & - c_2 \delta_3 U(\eta)^5 + k^2 (4 c_3 \kappa (\delta_{13} + \delta_{14}) - c_2 (\delta_6 + \delta_7)) U(\eta) U'(\eta)^2 - k^2 (a - 3 \kappa (2 c_2 \kappa \delta_3 + c_1 \delta_1)) U''(\eta) \\
 & + k^2 (-2 c_3 \kappa \delta_{14} - c_2 (\delta_4 + \delta_8)) U(\eta)^2 U''(\eta) - c_2 k^4 \delta_3 U^{(4)}(\eta) = 0.
 \end{aligned} \tag{15}$$

Eq. (15) can be simplified as

$$k^2 U^{(4)}(\eta) + \zeta_6 U(\eta)^2 U''(\eta) + \zeta_5 U'''(\eta) + \zeta_4 U(\eta) U'(\eta)^2 + \zeta_3 U(\eta)^5 + \zeta_2 U(\eta)^3 + \zeta_1 U(\eta) = 0, \tag{16}$$

where

$$\begin{aligned}
 \zeta_1 &= - \frac{a \kappa^2 + \kappa^3 (- (c_2 \kappa \delta_3 + c_1 \delta_1)) + \omega}{c_2 k^2 \delta_3}, \\
 \zeta_2 &= \frac{b - \kappa (\kappa (2 c_3 \kappa \delta_{14} + c_2 (\delta_4 - \delta_6 + \delta_7 + \delta_8)) + c_1 \delta_2)}{c_2 k^2 \delta_3}, \\
 \zeta_3 &= \frac{\delta_5}{k^2 \delta_3}, \quad \zeta_4 = \frac{c_2 (\delta_6 + \delta_7) - 4 c_3 \kappa (\delta_{13} + \delta_{14})}{c_2 \delta_3}, \\
 \zeta_5 &= \frac{a - 3 c_1 \kappa \delta_1}{c_2 \delta_3} - 6 \kappa^2, \quad \zeta_6 = \frac{2 c_3 \kappa \delta_{14} + c_2 (\delta_4 + \delta_8)}{c_2 \delta_3}.
 \end{aligned} \tag{17}$$

4. Integration algorithm

We may introduce a governing model with the form [6–10]:

$$F(\psi, \psi_x, \psi_t, \psi_{xt}, \psi_{xx}, \dots) = 0. \tag{18}$$

In this context, $\psi = \psi(x, t)$ characterizes a waveform, with x as the spatial coordinate and t as the temporal coordinate. By using waveform

$$\psi(x, t) = U(\eta), \quad \eta = k(x - vt), \quad (19)$$

we can reduce Eq. (18) to

$$P(U(\eta), -kvU'(\eta), kU'(\eta), k^2U''(\eta), \dots) = 0. \quad (20)$$

Here, v represents the wave velocity, η is the wave variable, and k signifies the wave width. To start the method, proceed with the following steps:

Step 1 Eq. (20) holds the solution structure:

$$U(\eta) = \Theta_0 + \sum_{i=1}^N \Theta_i \vartheta(\eta)^i, \quad (21)$$

with

$$\vartheta'(\eta)^2 = \sum_{l=0}^4 \sigma_l \vartheta(\eta)^l, \quad \sigma_4 \neq 0. \quad (22)$$

Here σ_l ($l = 0, 1, 2, 3, 4$) are constants. Equ. (22) offers various solutions:

Set-1: Bright soliton emerge for $\sigma_0 = \sigma_1 = \sigma_3 = 0$, $\sigma_2 > 0$, $\sigma_4 < 0$, $\sigma_2 > 0$, and $\sigma_4 > 0$:

$$\vartheta(\eta) = \sqrt{-\frac{\sigma_2}{\sigma_4}} \operatorname{sech}[\sqrt{\sigma_2} \eta], \quad \sigma_2 > 0, \quad \sigma_4 < 0, \quad (23)$$

$$\vartheta(\eta) = \sqrt{\frac{\sigma_2}{\sigma_4}} \operatorname{csch}[\sqrt{\sigma_2} \eta], \quad \sigma_2 > 0, \quad \sigma_4 > 0. \quad (24)$$

Set-2: Dark and singular solitons occur when $\sigma_2 < 0$, $\sigma_4 > 0$, $\sigma_0 = \frac{\sigma_2^2}{4\sigma_4}$ and $\sigma_1 = \sigma_3 = 0$:

$$\vartheta(\eta) = \sqrt{-\frac{\sigma_2}{2\sigma_4}} \tanh\left[\sqrt{-\frac{\sigma_2}{2}} \eta\right], \quad \sigma_2 < 0, \quad \sigma_4 > 0, \quad (25)$$

$$\vartheta(\eta) = \sqrt{-\frac{\sigma_2}{2\sigma_4}} \coth\left[\sqrt{-\frac{\sigma_2}{2}} \eta\right], \quad \sigma_2 < 0, \quad \sigma_4 > 0. \quad (26)$$

Set-3: Jacobi elliptic doubly periodic type solutions emerge for $\sigma_1 = \sigma_3 = 0$:

$$\vartheta(\eta) = \pm \sqrt{-\frac{\tau^2 \sigma_2}{(2\tau^2 - 1) \sigma_4}} \operatorname{cn} \left(\sqrt{\frac{\sigma_2}{2\tau^2 - 1}} \eta \middle| \tau \right); \sigma_0 = \frac{\tau^2 (1 - \tau^2) \sigma_2^2}{(2\tau^2 - 1)^2 \sigma_4}, \quad (27)$$

$$\vartheta(\eta) = \pm \sqrt{-\frac{\tau^2 \sigma_2}{(2 - \tau^2) \sigma_4}} \operatorname{dn} \left(\sqrt{\frac{\sigma_2}{2 - \tau^2}} \eta \middle| \tau \right); \sigma_0 = \frac{(1 - \tau^2) \sigma_2^2}{(2 - \tau^2)^2 \sigma_4}, \quad (28)$$

$$\vartheta(\eta) = \pm \sqrt{-\frac{\tau^2 \sigma_2}{(\tau^2 + 1) \sigma_4}} \operatorname{sn} \left(\sqrt{-\frac{\sigma_2}{\tau^2 + 1}} \eta \middle| \tau \right); \sigma_0 = \frac{\tau^2 \sigma_2^2}{(\tau^2 + 1)^2 \sigma_4}. \quad (29)$$

Here τ is set to be a real number between 0 and 1.

Set-4: Weierstrass elliptic doubly periodic type solutions arise for $\sigma_1 = \sigma_3 = 0$:

$$\vartheta(\eta) = \frac{3\wp'(\eta; g_2, g_3)}{\sqrt{\sigma_4} [6\wp(\eta; g_2, g_3) + \sigma_2]}, \sigma_4 > 0, \quad (30)$$

$$\vartheta(\eta) = \frac{\sqrt{\sigma_0} [6\wp(\eta; g_2, g_3) + \sigma_2]}{3\wp'(\eta; g_2, g_3)}, \sigma_0 > 0, \quad (31)$$

where the invariants of the Weierstrass elliptic function are derived from $g_2 = \frac{\sigma_2^2}{12} + \sigma_0 \sigma_4$ and $g_3 = \frac{\sigma_2}{216} (36\sigma_0 \sigma_4 - \sigma_2^2)$.

Set-5: Straddled solitons are identified by setting $\sigma_0 = \sigma_1 = 0$, and $\sigma_2 > 0$:

$$\vartheta(\eta) = \frac{-\sigma_2 \operatorname{sech}^2 \left[\frac{1}{2} \sqrt{\sigma_2} \eta \right]}{\pm 2\sqrt{\sigma_2 \sigma_4} \tanh \left[\frac{1}{2} \sqrt{\sigma_2} \eta \right] + \sigma_3}, \sigma_4 > 0, \quad (32)$$

$$\vartheta(\eta) = \frac{\sigma_2 \operatorname{csch}^2 \left[\frac{1}{2} \sqrt{\sigma_2} \eta \right]}{\pm 2\sqrt{\sigma_2 \sigma_4} \coth \left[\frac{1}{2} \sqrt{\sigma_2} \eta \right] + \sigma_3}, \sigma_4 > 0, \quad (33)$$

$$\vartheta(\eta) = \frac{2\sigma_2 \operatorname{sech} [\sqrt{\sigma_2} \eta]}{\pm \sqrt{\sigma_3^2 - 4\sigma_2 \sigma_4} - \sigma_3 \operatorname{sech} [\sqrt{\sigma_2} \eta]}, \sigma_3^2 - 4\sigma_2 \sigma_4 > 0, \quad (34)$$

$$\vartheta(\eta) = \frac{2\sigma_2 \operatorname{csch} [\sqrt{\sigma_2} \eta]}{\pm \sqrt{4\sigma_2 \sigma_4 - \sigma_3^2} - \sigma_3 \operatorname{csch} [\sqrt{\sigma_2} \eta]}, \sigma_3^2 - 4\sigma_2 \sigma_4 < 0, \quad (35)$$

$$\vartheta(\eta) = -\frac{\sigma_2\sigma_3\operatorname{sech}^2\left[\frac{\sqrt{\sigma_2}}{2}\eta\right]}{\sigma_3^2 - \sigma_2\sigma_4\left(1 - \tanh\left[\frac{\sqrt{\sigma_2}}{2}\eta\right]\right)^2}, \quad \sigma_3 \neq 0, \quad (36)$$

$$\vartheta(\eta) = \frac{\sigma_2\sigma_3\operatorname{csch}^2\left[\frac{\sqrt{\sigma_2}}{2}\eta\right]}{\sigma_3^2 - \sigma_2\sigma_4\left(1 - \coth\left[\frac{\sqrt{\sigma_2}}{2}\eta\right]\right)^2}, \quad \sigma_3 \neq 0. \quad (37)$$

Step 2 The parameter N in Eq. (21) is identified by balancing the nonlinear terms and the highest-order derivative in Eq. (20).

Step 3 Substitute Eq. (21) into Eq. (20), along with Eq. (22). This substitution leads to a polynomial in $\vartheta(\eta)$. By collecting terms with the same powers and setting them to zero, we derive an over-determined system of algebraic equations. This system can be solved to determine the parameters in Eqs. (19) and (22), ultimately yielding the solutions of Eq. (18).

5. Application to the model

In Eq. (16), the balance between $U^{(4)}(\eta)$ and $U(\eta)^5$ leads to $N = 1$. The solution follows the format outlined in this article's proposed technique:

$$U(\eta) = \Theta_0 + \Theta_1\vartheta(\eta). \quad (38)$$

The following system of algebraic equations is recovered when Eqs. (38) and (22) are substituted into Eq. (16):

$$\vartheta(\eta)^5 : \Theta_1^3\sigma_4\zeta_4 + 2\Theta_1^3\sigma_4\zeta_6 + \Theta_1^5\zeta_3 + 24\Theta_1\sigma_4^2k^2 = 0, \quad (39)$$

$$\vartheta(\eta)^4 : \Theta_1^3\sigma_3\zeta_4 + \frac{3}{2}\Theta_1^3\sigma_3\zeta_6 + \Theta_0\Theta_1^2\sigma_4\zeta_4 + 4\Theta_0\Theta_1^2\sigma_4\zeta_6 + 5\Theta_0\Theta_1^4\zeta_3 + 30\Theta_1\sigma_3\sigma_4k^2 = 0, \quad (40)$$

$$\vartheta(\eta)^3 : \Theta_1^3\sigma_2\zeta_4 + \Theta_1^3\sigma_2\zeta_6 + \Theta_0\Theta_1^2\sigma_3\zeta_4 + 3\Theta_0\Theta_1^2\sigma_3\zeta_6 + 2\Theta_1\sigma_4\zeta_5 + 2\Theta_0^2\Theta_1\sigma_4\zeta_6 + \Theta_1^3\zeta_2 \quad (41)$$

$$+ 10\Theta_0^2\Theta_1^3\zeta_3 + \frac{15}{2}\Theta_1\sigma_3^2k^2 + 20\Theta_1\sigma_2\sigma_4k^2 = 0, \quad (42)$$

$$\vartheta(\eta)^2 : \frac{3}{2}\Theta_1\Theta_0^2\sigma_3\zeta_6 + \Theta_1^2\Theta_0\sigma_2\zeta_4 + 2\Theta_1^2\Theta_0\sigma_2\zeta_6 + \Theta_1^3\sigma_1\zeta_4 + \frac{3}{2}\Theta_1\sigma_3\zeta_5 + \frac{1}{2}\Theta_1^3\sigma_1\zeta_6 + 10\Theta_1^2\Theta_0^3\zeta_3 \quad (43)$$

$$+ 3\Theta_1^2\Theta_0\zeta_2 + \frac{15}{2}\Theta_1\sigma_2\sigma_3k^2 + 15\Theta_1\sigma_1\sigma_4k^2 = 0, \quad (44)$$

$$\vartheta(\eta)^1 : \Theta_1 \Theta_0^2 \sigma_2 \zeta_6 + \Theta_1^2 \Theta_0 \sigma_1 \zeta_4 + \Theta_1^2 \Theta_0 \sigma_1 \zeta_6 + \Theta_1^3 \sigma_0 \zeta_4 + \Theta_1 \sigma_2 \zeta_5 + 5 \Theta_1 \Theta_0^4 \zeta_3 + 3 \Theta_1 \Theta_0^2 \zeta_2 + \Theta_1 \zeta_1 \quad (45)$$

$$+ \Theta_1 \sigma_2^2 k^2 + \frac{9}{2} \Theta_1 \sigma_1 \sigma_3 k^2 + 12 \Theta_1 \sigma_0 \sigma_4 k^2 = 0, \quad (46)$$

$$\vartheta(\eta)^0 : \frac{1}{2} \Theta_1 \Theta_0^2 \sigma_1 \zeta_6 + \Theta_1^2 \Theta_0 \sigma_0 \zeta_4 + \frac{1}{2} \Theta_1 \sigma_1 \zeta_5 + \Theta_0^5 \zeta_3 + \Theta_0^3 \zeta_2 + \Theta_0 \zeta_1 + \frac{1}{2} \Theta_1 \sigma_1 \sigma_2 k^2 \quad (47)$$

$$+ 3 \Theta_1 \sigma_0 \sigma_3 k^2 = 0. \quad (48)$$

The following cases are derived after solving these equations:

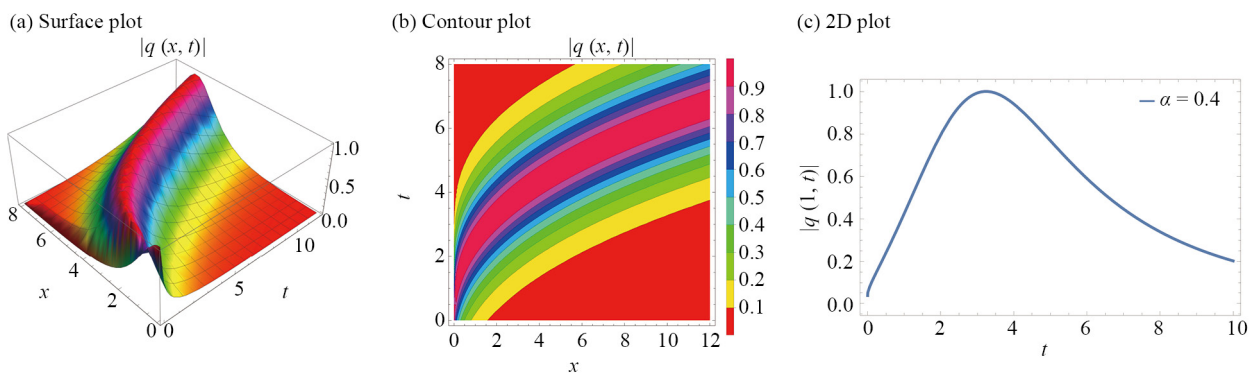
Case 1 Choosing $\sigma_0 = \sigma_1 = \sigma_3 = 0$, yields

$$\Theta_0 = 0, \quad \Theta_1 = \sqrt{\frac{2\sigma_4(9\zeta_5\sigma_2 + 10\zeta_1)}{\sigma_2((\zeta_4 + \zeta_6)\sigma_2 + \zeta_2)}}, \quad k = \frac{\sqrt{-(\zeta_5\sigma_2 + \zeta_1)}}{\sigma_2},$$

$$\zeta_3 = \frac{((\zeta_4 + \zeta_6)\sigma_2 + \zeta_2)(3\zeta_5\sigma_2((\zeta_4 - 2\zeta_6)\sigma_2 + 4\zeta_2) + 2\zeta_1((\zeta_4 - 4\zeta_6)\sigma_2 + 6\zeta_2))}{2(9\zeta_5\sigma_2 + 10\zeta_1)^2}. \quad (49)$$

The solutions of Eq. (1) are achieved as a consequence:

$$q(x, t) = \pm \sqrt{-\frac{2(9\zeta_5\sigma_2 + 10\zeta_1)}{(\zeta_4 + \zeta_6)\sigma_2 + \zeta_2}} \operatorname{sech} \left[\sqrt{-\frac{\zeta_5\sigma_2 + \zeta_1}{\sigma_2}} \left(x - v \frac{t^\alpha}{\alpha} \right) \right] e^{i(-\kappa x + \omega \frac{t^\alpha}{\alpha} + \vartheta_0)}. \quad (50)$$



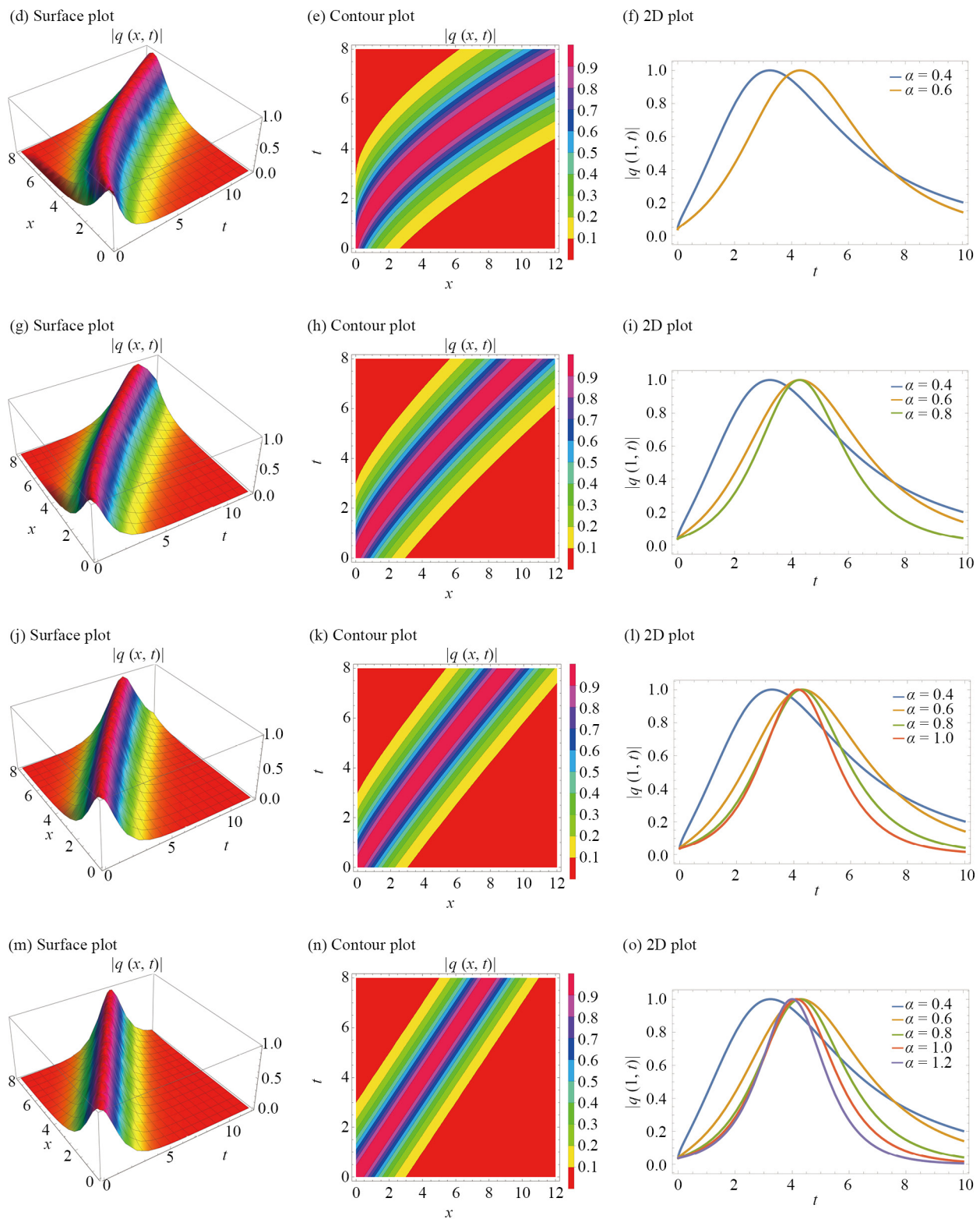


Figure 1. Exploring the features of a bright soliton, particularly its magnitude

Eq. (50) is a bright soliton with $(\zeta_5 \sigma_2 + \zeta_1) \sigma_2 < 0$, and $(9\zeta_5 \sigma_2 + 10\zeta_1)((\zeta_4 + \zeta_6) \sigma_2 + \zeta_2) < 0$:

$$q(x, t) = \pm \sqrt{\frac{2(9\zeta_5 \sigma_2 + 10\zeta_1)}{(\zeta_4 + \zeta_6) \sigma_2 + \zeta_2}} \operatorname{csch} \left[\sqrt{-\frac{\zeta_5 \sigma_2 + \zeta_1}{\sigma_2}} \left(x - v \frac{t^\alpha}{\alpha} \right) \right] e^{i(-\kappa x + \omega \frac{t^\alpha}{\alpha} + \vartheta_0)}. \quad (51)$$

Eq. (51) is a singular soliton with $(\zeta_5 \sigma_2 + \zeta_1) \sigma_2 < 0$, and $(9\zeta_5 \sigma_2 + 10\zeta_1)((\zeta_4 + \zeta_6) \sigma_2 + \zeta_2) > 0$.

Case 2 Choosing $\sigma_0 = \frac{\sigma_2^2}{4\sigma_4}$, $\sigma_1 = \sigma_3 = 0$, yields

$$\begin{aligned} \Theta_0 &= 0, \quad \Theta_1 = \sqrt{\frac{2\sigma_4(3\zeta_5 \sigma_2 + 5\zeta_1)}{\sigma_2(4\zeta_2 - (\zeta_4 - 4\zeta_6) \sigma_2)}}, \\ \zeta_3 &= \frac{(4\zeta_2 - (\zeta_4 - 4\zeta_6) \sigma_2)(6\zeta_2 \zeta_5 \sigma_2 + \zeta_1((\zeta_4 - 4\zeta_6) \sigma_2 + 6\zeta_2))}{4(3\zeta_5 \sigma_2 + 5\zeta_1)^2}, \\ k &= \sqrt{\frac{-2\zeta_1((\zeta_4 + \zeta_6) \sigma_2 + \zeta_2) - \zeta_5 \sigma_2((\zeta_4 + 2\zeta_6) \sigma_2 + 2\zeta_2)}{2\sigma_2^2(4\zeta_2 - (\zeta_4 - 4\zeta_6) \sigma_2)}}. \end{aligned} \quad (52)$$

Dark and singular solitons emerge by setting $(3\zeta_5 \sigma_2 + 5\zeta_1)((\zeta_4 - 4\zeta_6) \sigma_2 - 4\zeta_2) > 0$, and $\sigma_2(4\zeta_2 - (\zeta_4 - 4\zeta_6) \sigma_2)(2\zeta_1((\zeta_4 + \zeta_6) \sigma_2 + \zeta_2) + \zeta_5 \sigma_2((\zeta_4 + 2\zeta_6) \sigma_2 + 2\zeta_2)) > 0$:

$$\begin{aligned} q(x, t) &= \pm \sqrt{\frac{2(3\zeta_5 \sigma_2 + 5\zeta_1)}{(\zeta_4 - 4\zeta_6) \sigma_2 - 4\zeta_2}} \\ &\times \tanh \left[\frac{1}{2} \sqrt{\frac{2\zeta_1((\zeta_4 + \zeta_6) \sigma_2 + \zeta_2) + \zeta_5 \sigma_2((\zeta_4 + 2\zeta_6) \sigma_2 + 2\zeta_2)}{\sigma_2(4\zeta_2 - (\zeta_4 - 4\zeta_6) \sigma_2)}} \left(x - v \frac{t^\alpha}{\alpha} \right) \right] \\ &\times e^{i(-\kappa x + \omega \frac{t^\alpha}{\alpha} + \vartheta_0)}, \end{aligned} \quad (53)$$

$$\begin{aligned} q(x, t) &= \pm \sqrt{\frac{2(3\zeta_5 \sigma_2 + 5\zeta_1)}{(\zeta_4 - 4\zeta_6) \sigma_2 - 4\zeta_2}} \\ &\times \coth \left[\frac{1}{2} \sqrt{\frac{2\zeta_1((\zeta_4 + \zeta_6) \sigma_2 + \zeta_2) + \zeta_5 \sigma_2((\zeta_4 + 2\zeta_6) \sigma_2 + 2\zeta_2)}{\sigma_2(4\zeta_2 - (\zeta_4 - 4\zeta_6) \sigma_2)}} \left(x - v \frac{t^\alpha}{\alpha} \right) \right] \\ &\times e^{i(-\kappa x + \omega \frac{t^\alpha}{\alpha} + \vartheta_0)}. \end{aligned} \quad (54)$$

Case 3 $\sigma_1 = \sigma_3 = 0$.

$$(i) \sigma_0 = \frac{\tau^2 (1 - \tau^2) \sigma_2^2}{(2\tau^2 - 1)^2 \sigma_4},$$

$$\Theta_0 = 0, \Theta_1 = \sqrt{\frac{\sigma_4 (18\zeta_5 \sigma_2 + 20\zeta_1)}{\sigma_2 ((\zeta_4 + \zeta_6) \sigma_2 + \zeta_2)}},$$

$$\zeta_3 = \frac{(\sigma_2 (\zeta_4 \tau_2 + \zeta_6 \tau_1) + \zeta_2 \tau_1) (2\zeta_1 \tau_4^2 ((\zeta_4 - 4\zeta_6) \sigma_2 + 6\zeta_2) + 3\zeta_5 \sigma_2 ((\zeta_4 - 2\zeta_6) \tau_1 \sigma_2 + 4\zeta_2 \tau_4^2))}{2 (3\zeta_5 (5 - 2\tau_1) \sigma_2 + 10\zeta_1 \tau_4^2)^2},$$

$$k = \sqrt{-\frac{\zeta_1 \tau_4^2 ((\zeta_4 + \zeta_6) \sigma_2 + \zeta_2) + \zeta_5 \sigma_2 (\sigma_2 (\zeta_6 \tau_4^2 + \zeta_4 \tau_3) + \zeta_2 \tau_4^2)}{\sigma_2^2 (\zeta_4 \sigma_2 + \sigma_2 (\zeta_6 + 4 (3\zeta_4 - 2\zeta_6) (\tau^2 - 1) \tau^2) + \zeta_2 \tau_1)}}, \quad (55)$$

where $\tau_1 = -8\tau^4 + 8\tau^2 + 1$, $\tau_2 = 12\tau^4 - 12\tau^2 + 1$, $\tau_3 = 6\tau^4 - 6\tau^2 + 1$, $\tau_4 = 1 - 2\tau^2$. Thus, Eq. (1) holds the waveform:

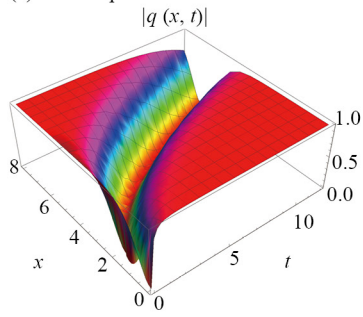
$$\begin{aligned} q(x, t) = & \pm \sqrt{-\frac{2\tau^2 (9\zeta_5 \sigma_2 + 10\zeta_1)}{(2\tau^2 - 1) ((\zeta_4 + \zeta_6) \sigma_2 + \zeta_2)}} \\ & \times \operatorname{cn} \left(\sqrt{\frac{\zeta_1 \tau_4^2 ((\zeta_4 + \zeta_6) \sigma_2 + \zeta_2) + \zeta_5 \sigma_2 (\sigma_2 (\zeta_6 \tau_4^2 + \zeta_4 \tau_3) + \zeta_2 \tau_4^2)}{\tau_4 \sigma_2 (\zeta_4 \sigma_2 + \sigma_2 (\zeta_6 + 4 (3\zeta_4 - 2\zeta_6) (\tau^2 - 1) \tau^2) + \zeta_2 \tau_1)}} \left(x - v \frac{t^\alpha}{\alpha} \right) \middle| \tau \right) \\ & \times e^{i \left(-\kappa x + \omega \frac{t^\alpha}{\alpha} + \vartheta_0 \right)}. \end{aligned} \quad (56)$$

A bright soliton is recovered when $\tau \rightarrow 1^-$ in Eq. (56):

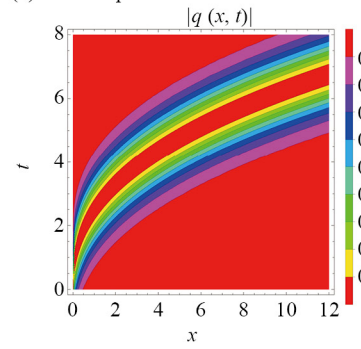
$$\begin{aligned} q(x, t) = & \pm \sqrt{-\frac{2 (9\zeta_5 \sigma_2 + 10\zeta_1)}{(\zeta_4 + \zeta_6) \sigma_2 + \zeta_2}} \\ & \times \operatorname{sech} \left[\sqrt{-\frac{\zeta_1 ((\zeta_4 + \zeta_6) \sigma_2 + \zeta_2) + \zeta_5 \sigma_2 ((\zeta_4 + \zeta_6) \sigma_2 + \zeta_2)}{\sigma_2 (\zeta_4 \sigma_2 + \zeta_6 \sigma_2 + \zeta_2)}} \left(x - v \frac{t^\alpha}{\alpha} \right) \right] \\ & \times e^{i \left(-\kappa x + \omega \frac{t^\alpha}{\alpha} + \vartheta_0 \right)}. \end{aligned} \quad (57)$$

Provided that $(9\zeta_5 \sigma_2 + 10\zeta_1) ((\zeta_4 + \zeta_6) \sigma_2 + \zeta_2) < 0$, and $\sigma_2 (\zeta_4 \sigma_2 + \zeta_6 \sigma_2 + \zeta_2) (\zeta_1 ((\zeta_4 + \zeta_6) \sigma_2 + \zeta_2) + \zeta_5 \sigma_2 ((\zeta_4 + \zeta_6) \sigma_2 + \zeta_2)) < 0$.

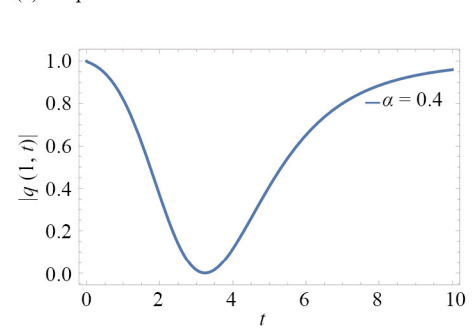
(a) Surface plot



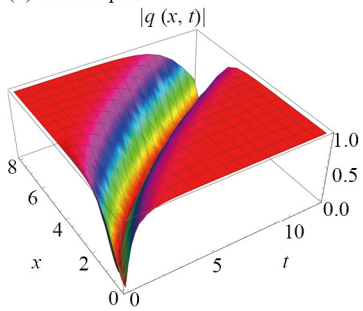
(b) Contour plot



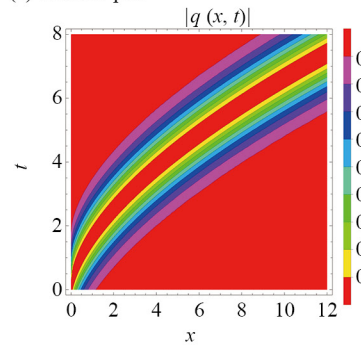
(c) 2D plot



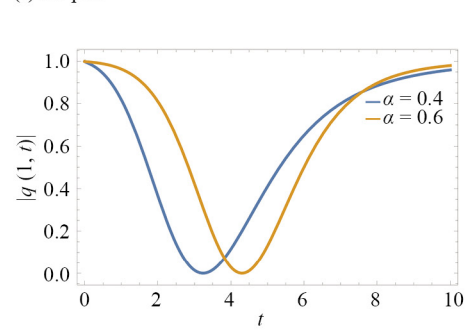
(d) Surface plot



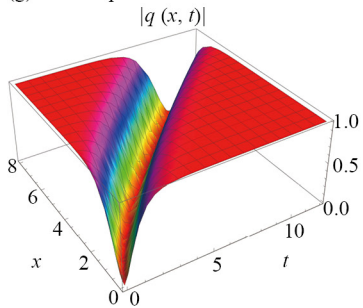
(e) Contour plot



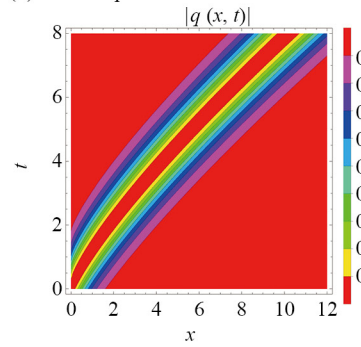
(f) 2D plot



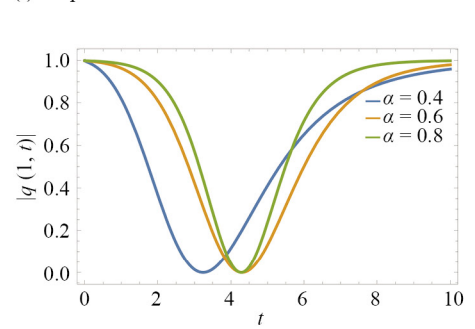
(g) Surface plot



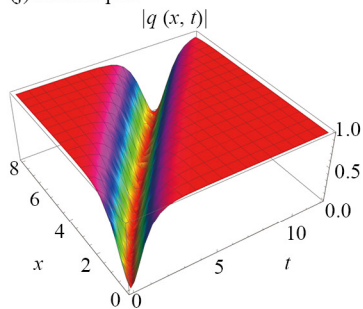
(h) Contour plot



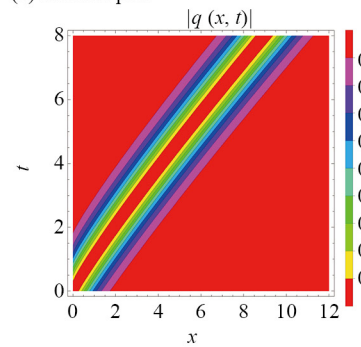
(i) 2D plot



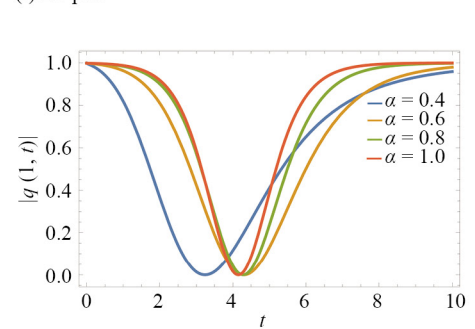
(j) Surface plot



(k) Contour plot



(l) 2D plot



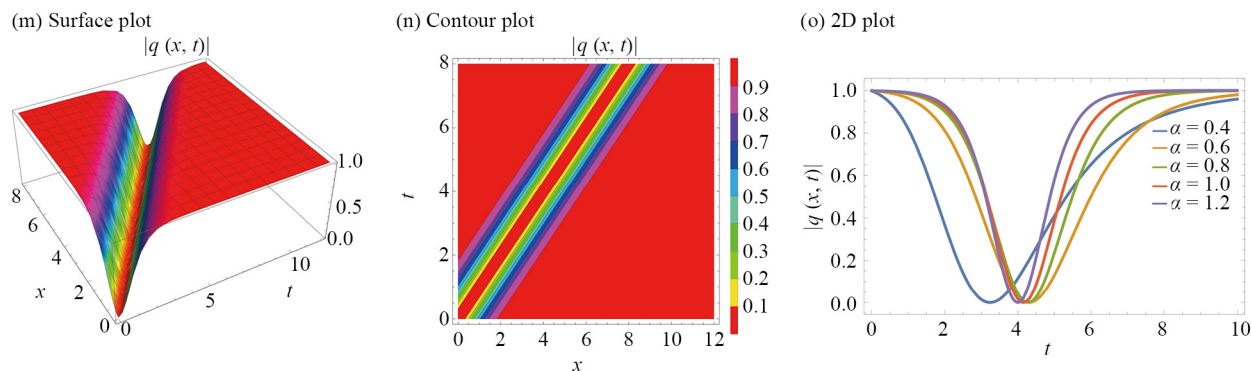


Figure 2. Examining the characteristics exhibited by a dark soliton, including its magnitude

$$\begin{aligned}
 \text{(ii)} \quad \sigma_0 &= \frac{\tau^2 (1 - \tau^2) \sigma_2^2}{(2\tau^2 - 1)^2 \sigma_4}, \\
 \Theta_0 &= 0, \quad \Theta_1 = \sqrt{\frac{\sigma_4 (6\zeta_5 (5\tau^4 - 2\tau_7) \sigma_2 + 20\zeta_1 \tau_6^2)}{\sigma_2 (\sigma_2 (\zeta_4 \tau_7 + \zeta_6 \tau_5) + \zeta_2 \tau_5)}}, \\
 \zeta_3 &= \frac{(\sigma_2 (\zeta_4 \tau_7 + \zeta_6 \tau_5) + \zeta_2 \tau_5) (3\zeta_5 \sigma_2 ((\zeta_4 - 2\zeta_6) \tau^4 \sigma_2 + 4\zeta_2 \tau_6^2) + 2\zeta_1 \tau_6^2 ((\zeta_4 - 4\zeta_6) \sigma_2 + 6\zeta_2))}{2(3\zeta_5 (5\tau^4 - 2\tau_7) \sigma_2 + 10\zeta_1 \tau_6^2)^2}, \\
 k &= \sqrt{\frac{\zeta_1 (-\tau_6^2) ((\zeta_4 + \zeta_6) \sigma_2 + \zeta_2) - \zeta_5 \sigma_2 (\sigma_2 (\zeta_4 (\tau^4 - 2\tau^2 + 2) + \zeta_6 \tau_6^2) + \zeta_2 \tau_6^2)}{\sigma_2^2 (\sigma_2 (\zeta_4 \tau_7 + \zeta_6 \tau_5) + \zeta_2 \tau_5)}}, \quad (58)
 \end{aligned}$$

where $\tau_7 = \tau^4 + 4\tau^2 - 4$, $\tau_6 = \tau^2 - 2$, $\tau_5 = \tau^4 - 16\tau^2 + 16$. Due to this, the following solutions for Eq. (1) are achieved:

$$\begin{aligned}
 q(x, t) &= \pm \sqrt{\frac{2\tau^2 (3\zeta_5 (5\tau^4 - 2\tau_7) \sigma_2 + 10\zeta_1 \tau_6^2)}{(\tau^2 - 2) (\zeta_4 \tau_7 \sigma_2 + \tau_5 (\zeta_6 \sigma_2 + \zeta_2))}} \\
 &\times \operatorname{dn} \left(\sqrt{\frac{\zeta_4 \zeta_5 (\tau^4 - 2\tau^2 + 2) \sigma_2^2 + \tau_6^2 (\zeta_5 \sigma_2 (\zeta_6 \sigma_2 + \zeta_2) + \zeta_1 ((\zeta_4 + \zeta_6) \sigma_2 + \zeta_2))}{\tau_6 \sigma_2 (\zeta_4 \tau_7 \sigma_2 + \tau_5 (\zeta_6 \sigma_2 + \zeta_2))}} \left(x - v \frac{t^\alpha}{\alpha} \right) \middle| \tau \right) \\
 &\times e^{i(-\kappa x + \omega \frac{t^\alpha}{\alpha} + \vartheta_0)}. \quad (59)
 \end{aligned}$$

A bright soliton is extracted when $\tau \rightarrow 1^-$ in Eq. (59):

$$q(x, t) = \pm \sqrt{-\frac{2(9\zeta_5 \sigma_2 + 10\zeta_1)}{(\zeta_4 + \zeta_6) \sigma_2 + \zeta_2}} \operatorname{sech} \left[\sqrt{-\frac{\zeta_5 \sigma_2 + \zeta_1}{\sigma_2}} \left(x - v \frac{t^\alpha}{\alpha} \right) \right] \times e^{i(-\kappa x + \omega \frac{t^\alpha}{\alpha} + \vartheta_0)}, \quad (60)$$

provided that $(9\zeta_5\sigma_2 + 10\zeta_1)((\zeta_4 + \zeta_6)\sigma_2 + \zeta_2) < 0$, and $\sigma_2(\zeta_5\sigma_2 + \zeta_1) < 0$.

$$(iii) \sigma_0 = \frac{\tau^2 \sigma_2^2}{(\tau^2 + 1)^2 \sigma_4},$$

$$\Theta_0 = 0, \Theta_1 = \sqrt{\frac{\sigma_4 (6\zeta_5 \tau_{11} \sigma_2 + 20\zeta_1 \tau_9^2)}{\sigma_2 (\sigma_2 (\zeta_4 \tau_{10} + \zeta_6 \tau_8) + \zeta_2 \tau_8)}},$$

$$\zeta_3 = \frac{(\zeta_4 \tau_{10} \sigma_2 + \tau_8 (\zeta_6 \sigma_2 + \zeta_2)) \left(3\zeta_5 (\zeta_4 - 2\zeta_6) (\tau^2 - 1)^2 \sigma_2^2 + 2\tau_9^2 (6\zeta_2 \zeta_5 \sigma_2 + \zeta_1 ((\zeta_4 - 4\zeta_6) \sigma_2 + 6\zeta_2)) \right)}{2 (3\zeta_5 \tau_{11} \sigma_2 + 10\zeta_1 \tau_9^2)^2},$$

$$k = \sqrt{\frac{-\tau_9^2 \zeta_1 ((\zeta_4 + \zeta_6) \sigma_2 + \zeta_2) - \zeta_5 \sigma_2 (\sigma_2 (\zeta_4 (\tau^4 + 1) + \zeta_6 \tau_9^2) + \zeta_2 \tau_9^2)}{\sigma_2^2 (\sigma_2 (\zeta_4 \tau_{10} + \zeta_6 \tau_8) + \zeta_2 \tau_8)}}, \quad (61)$$

where $\tau_{11} = 3\tau^4 + 2\tau^2 + 3$, $\tau_{10} = \tau^4 - 6\tau^2 + 1$, $\tau_9 = \tau^2 + 1$, $\tau_8 = \tau^4 + 14\tau^2 + 1$. The following solutions for Eq. (1) are derived as a consequence:

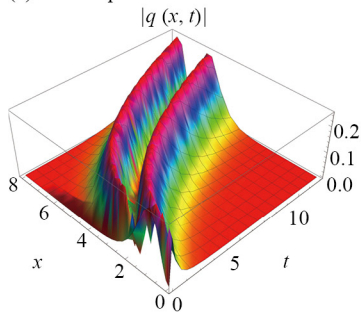
$$\begin{aligned} q(x, t) = & \pm \sqrt{-\frac{2\tau^2 (3\zeta_5 (3\tau^4 + 2\tau^2 + 3) \sigma_2 + 10\zeta_1 \tau_9^2)}{\tau_9 (\zeta_4 \tau_{10} \sigma_2 + \tau_8 (\zeta_6 \sigma_2 + \zeta_2))}} \\ & \times \operatorname{sn} \left(\sqrt{\frac{\zeta_4 \zeta_5 (\tau^4 + 1) \sigma_2^2 + \tau_9^2 (\zeta_5 \sigma_2 (\zeta_6 \sigma_2 + \zeta_2) + \zeta_1 ((\zeta_4 + \zeta_6) \sigma_2 + \zeta_2))}{\tau_9 \sigma_2 (\zeta_4 \tau_{10} \sigma_2 + \tau_8 (\zeta_6 \sigma_2 + \zeta_2))}} \left(x - v \frac{t^\alpha}{\alpha} \right) \middle| \tau \right) \\ & \times e^{i(-\kappa x + \omega \frac{t^\alpha}{\alpha} + \vartheta_0)}. \end{aligned} \quad (62)$$

A dark soliton is derived when $\tau \rightarrow 1^-$ in Eq. (62):

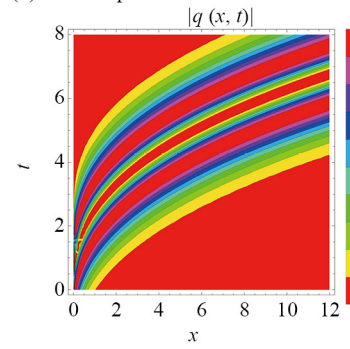
$$\begin{aligned} q(x, t) = & \pm \sqrt{-\frac{24\zeta_5 \sigma_2 + 40\zeta_1}{16(\zeta_6 \sigma_2 + \zeta_2) - 4\zeta_4 \sigma_2}} \\ & \times \tanh \left[\sqrt{\frac{2\zeta_4 \zeta_5 \sigma_2^2 + 4(\zeta_5 \sigma_2 (\zeta_6 \sigma_2 + \zeta_2) + \zeta_1 ((\zeta_4 + \zeta_6) \sigma_2 + \zeta_2))}{2\sigma_2 (16(\zeta_6 \sigma_2 + \zeta_2) - 4\zeta_4 \sigma_2)}} \left(x - v \frac{t^\alpha}{\alpha} \right) \right] \\ & \times e^{i(-\kappa x + \omega \frac{t^\alpha}{\alpha} + \vartheta_0)}, \end{aligned} \quad (63)$$

provided that $(24\zeta_5 \sigma_2 + 40\zeta_1)(16(\zeta_6 \sigma_2 + \zeta_2) - 4\zeta_4 \sigma_2) < 0$, and $\sigma_2 (16(\zeta_6 \sigma_2 + \zeta_2) - 4\zeta_4 \sigma_2) (2\zeta_4 \zeta_5 \sigma_2^2 + 4(\zeta_5 \sigma_2 (\zeta_6 \sigma_2 + \zeta_2) + \zeta_1 ((\zeta_4 + \zeta_6) \sigma_2 + \zeta_2))) > 0$.

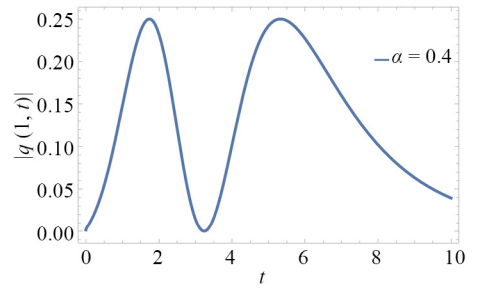
(a) Surface plot



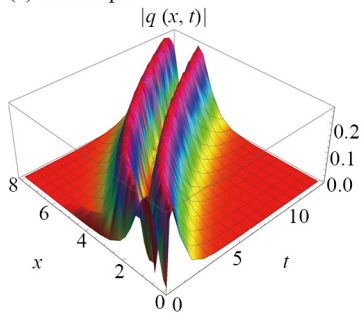
(b) Contour plot



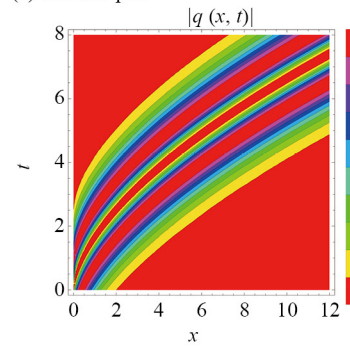
(c) 2D plot



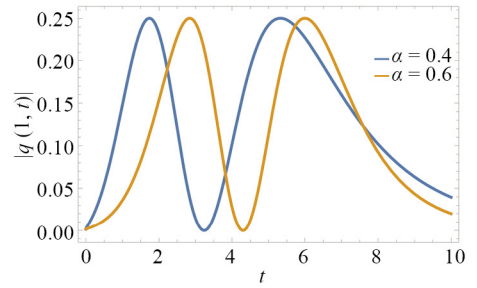
(d) Surface plot



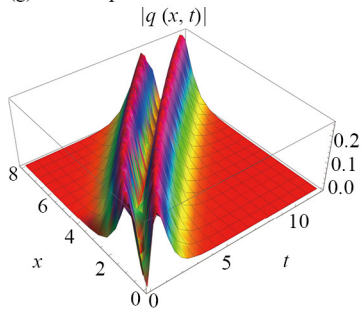
(e) Contour plot



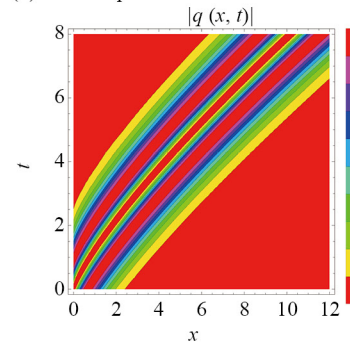
(f) 2D plot



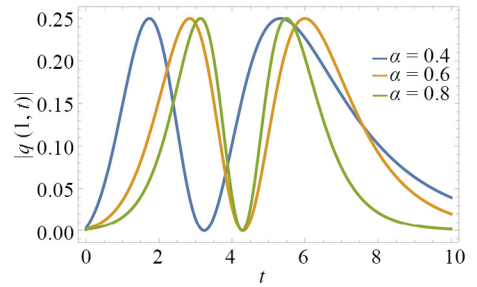
(g) Surface plot



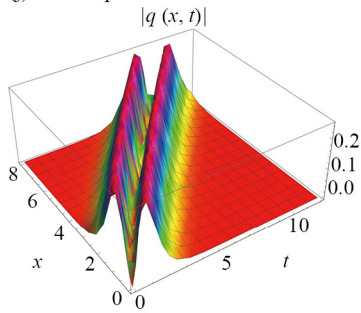
(h) Contour plot



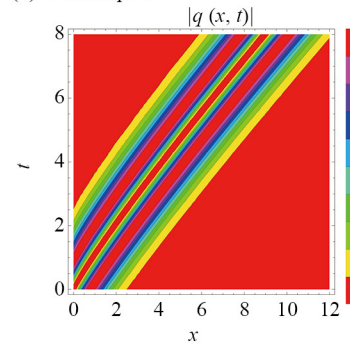
(i) 2D plot



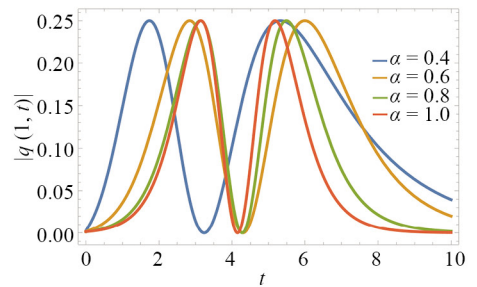
(j) Surface plot



(k) Contour plot



(l) 2D plot



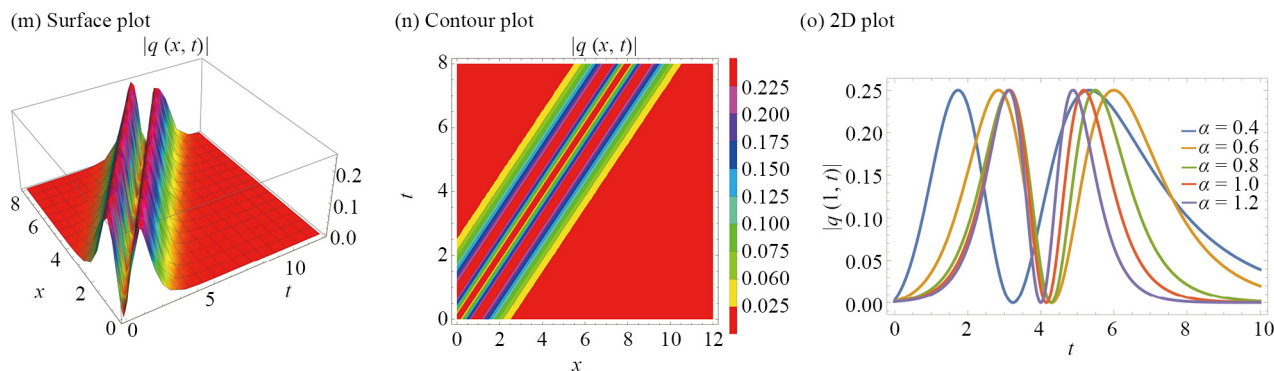


Figure 3. Examining the characteristics exhibited by a bright-dark straddled soliton, including its magnitude

Case 4 Choosing $\sigma_1 = \sigma_3 = 0$, yields

$$\Theta_0 = 0, \quad \Theta_1 = \frac{\sqrt{2\sigma_4} \sqrt{9\sigma_2^2 \zeta_5 + 10\sigma_2 \zeta_1 - 12\sigma_0 \sigma_4 \zeta_5}}{\sqrt{\sigma_2^3 (\zeta_4 + \zeta_6) + \sigma_2^2 \zeta_2 + 4\sigma_0 \sigma_4 \sigma_2 (3\zeta_6 - 2\zeta_4) + 12\sigma_0 \sigma_4 \zeta_2}},$$

$$k = \sqrt{\frac{\zeta_1 (\sigma_2 (\zeta_4 + \zeta_6) + \zeta_2) + \zeta_5 (\sigma_2^2 (\zeta_4 + \zeta_6) + \sigma_2 \zeta_2 - 2\sigma_0 \sigma_4 \zeta_4)}{-(\sigma_2^3 (\zeta_4 + \zeta_6)) + 4\sigma_0 \sigma_4 \sigma_2 (2\zeta_4 - 3\zeta_6) - \sigma_2^2 \zeta_2 - 12\sigma_0 \sigma_4 \zeta_2}},$$

$$\zeta_3 = \frac{\sigma_2^2 (3\sigma_2 \zeta_5 (\sigma_2 (\zeta_4 - 2\zeta_6) + 4\zeta_2) + 2\zeta_1 (\sigma_2 (\zeta_4 - 4\zeta_6) + 6\zeta_2)) (\sigma_2 (\zeta_4 + \zeta_6) + \zeta_2)}{2 (9\sigma_2^2 \zeta_5 + 10\sigma_2 \zeta_1 - 12\sigma_0 \sigma_4 \zeta_5)^2}. \quad (64)$$

This causes to the following solutions for Eq. (1):

$$q(x, t) = \sqrt{\frac{2 (9\sigma_2^2 \zeta_5 + 10\sigma_2 \zeta_1 - 12\sigma_0 \sigma_4 \zeta_5)}{\sigma_2^3 (\zeta_4 + \zeta_6) + \sigma_2^2 \zeta_2 + 4\sigma_0 \sigma_4 \sigma_2 (3\zeta_6 - 2\zeta_4) + 12\sigma_0 \sigma_4 \zeta_2}} \left\{ \frac{3\wp' \left(k \left(x - v \frac{t^\alpha}{\alpha} \right); g_2, g_3 \right)}{\left[6\wp \left(k \left(x - v \frac{t^\alpha}{\alpha} \right); g_2, g_3 \right) + \sigma_2 \right]} \right\}$$

$$\times e^{i \left(-\kappa x + \omega \frac{t^\alpha}{\alpha} + \vartheta_0 \right)}, \quad (65)$$

$$q(x, t) = \sqrt{\frac{2\sigma_0 (9\sigma_2^2 \zeta_5 + 10\sigma_2 \zeta_1 - 12\sigma_0 \sigma_4 \zeta_5)}{\sigma_2^3 (\zeta_4 + \zeta_6) + \sigma_2^2 \zeta_2 + 4\sigma_0 \sigma_4 \sigma_2 (3\zeta_6 - 2\zeta_4) + 12\sigma_0 \sigma_4 \zeta_2}} \left\{ \frac{\left[6\wp \left(k \left(x - v \frac{t^\alpha}{\alpha} \right); g_2, g_3 \right) + \sigma_2 \right]}{3\wp' \left(k \left(x - v \frac{t^\alpha}{\alpha} \right); g_2, g_3 \right)} \right\}$$

$$\times e^{i \left(-\kappa x + \omega \frac{t^\alpha}{\alpha} + \vartheta_0 \right)}. \quad (66)$$

A singular soliton is obtained by setting $\sigma_4 = 0$ in Eq. (65), provided $(9\zeta_5\sigma_2 + 10\zeta_1)((\zeta_4 + \zeta_6)\sigma_2 + \zeta_2) > 0$, and $\sigma_2(\zeta_5\sigma_2 + \zeta_1) < 0$:

$$q(x, t) = \sqrt{\frac{2(9\zeta_5\sigma_2 + 10\zeta_1)}{(\zeta_4 + \zeta_6)\sigma_2 + \zeta_2}} \operatorname{csch} \left[\sqrt{-\frac{\zeta_5\sigma_2 + \zeta_1}{\sigma_2}} \left(x - v\frac{t^\alpha}{\alpha} \right) \right] e^{i(-\kappa x + \omega\frac{t^\alpha}{\alpha} + \vartheta_0)}. \quad (67)$$

Case 5 Choosing $\sigma_0 = \sigma_1 = 0$, yields

$$\Theta_0 = 0, \Theta_1 = 2\sqrt{\frac{3\zeta_5\sigma_4}{(2\zeta_4 + 3\zeta_6)\sigma_2}}, \zeta_1 = -\frac{4}{5}\zeta_5\sigma_2, k = \sqrt{-\frac{\zeta_5}{5\sigma_2}}, \quad (68)$$

$$\zeta_2 = \frac{3\zeta_6(3\sigma_3^2 - 4\sigma_2\sigma_4) + 2\zeta_4(3\sigma_3^2 - 8\sigma_2\sigma_4)}{24\sigma_4}, \zeta_3 = -\frac{(2\zeta_4^2 + 11\zeta_6\zeta_4 + 12\zeta_6^2)\sigma_2}{60\zeta_5}.$$

This leads to the straddled solitons for Eq. (1):

$$q(x, t) = \left\{ \frac{2\sqrt{\frac{3\zeta_5\sigma_4\sigma_2}{2\zeta_4 + 3\zeta_6}} \operatorname{sech}^2 \left[\frac{1}{2}\sqrt{-\frac{\zeta_5}{5}} \left(x - v\frac{t^\alpha}{\alpha} \right) \right]}{\pm 2\sqrt{\sigma_2\sigma_4} \tanh \left[\frac{1}{2}\sqrt{-\frac{\zeta_5}{5}} \left(x - v\frac{t^\alpha}{\alpha} \right) \right] + \sigma_3} \right\} e^{i(-\kappa x + \omega\frac{t^\alpha}{\alpha} + \vartheta_0)}, \quad (69)$$

$$q(x, t) = \left\{ \frac{2\sqrt{\frac{3\zeta_5\sigma_4\sigma_2}{2\zeta_4 + 3\zeta_6}} \operatorname{csch}^2 \left[\frac{1}{2}\sqrt{-\frac{\zeta_5}{5}} \left(x - v\frac{t^\alpha}{\alpha} \right) \right]}{\pm 2\sqrt{\sigma_2\sigma_4} \coth \left[\frac{1}{2}\sqrt{-\frac{\zeta_5}{5}} \left(x - v\frac{t^\alpha}{\alpha} \right) \right] + \sigma_3} \right\} e^{i(-\kappa x + \omega\frac{t^\alpha}{\alpha} + \vartheta_0)}. \quad (70)$$

Setting $\sigma_3 = \pm 2\sqrt{\sigma_2\sigma_4}$ into Eqs. (69) and (70) yields

$$q(x, t) = \left\{ \frac{\mp \sqrt{\frac{3\zeta_5}{2\zeta_4 + 3\zeta_6}} \operatorname{sech}^2 \left[\frac{1}{2}\sqrt{-\frac{\zeta_5}{5}} \left(x - v\frac{t^\alpha}{\alpha} \right) \right]}{\tanh \left[\frac{1}{2}\sqrt{-\frac{\zeta_5}{5}} \left(x - v\frac{t^\alpha}{\alpha} \right) \right] + 1} \right\} e^{i(-\kappa x + \omega\frac{t^\alpha}{\alpha} + \vartheta_0)}, \quad (71)$$

$$q(x, t) = \left\{ \frac{\pm \sqrt{\frac{3\zeta_5}{2\zeta_4 + 3\zeta_6}} \operatorname{csch}^2 \left[\frac{1}{2}\sqrt{-\frac{\zeta_5}{5}} \left(x - v\frac{t^\alpha}{\alpha} \right) \right]}{\coth \left[\frac{1}{2}\sqrt{-\frac{\zeta_5}{5}} \left(x - v\frac{t^\alpha}{\alpha} \right) \right] + 1} \right\} e^{i(-\kappa x + \omega\frac{t^\alpha}{\alpha} + \vartheta_0)}, \quad (72)$$

provided that $\zeta_5 < 0$, and $2\zeta_4 + 3\zeta_6 < 0$.

A singular soliton emerges by applying $\sigma_3 = 0$ to Eqs. (69) and (70):

$$q(x, t) = \mp 2 \sqrt{\frac{3\zeta_5}{2\zeta_4 + 3\zeta_6}} \operatorname{csch} \left[\sqrt{-\frac{\zeta_5}{5}} \left(x - v \frac{t^\alpha}{\alpha} \right) \right] e^{i(-\kappa x + \omega \frac{t^\alpha}{\alpha} + \vartheta_0)}. \quad (73)$$

Another possible straddled solitons are obtained:

$$q(x, t) = \left\{ \frac{4 \sqrt{\frac{3\zeta_5 \sigma_4 \sigma_2}{2\zeta_4 + 3\zeta_6}} \operatorname{sech} \left[\sqrt{-\frac{\zeta_5}{5}} \left(x - v \frac{t^\alpha}{\alpha} \right) \right]}{\pm \sqrt{\sigma_3^2 - 4\sigma_2 \sigma_4} - \sigma_3 \operatorname{sech} \left[\sqrt{-\frac{\zeta_5}{5}} \left(x - v \frac{t^\alpha}{\alpha} \right) \right]} \right\} e^{i(-\kappa x + \omega \frac{t^\alpha}{\alpha} + \vartheta_0)}, \quad (74)$$

$$q(x, t) = \left\{ \frac{4 \sqrt{\frac{3\zeta_5 \sigma_4 \sigma_2}{2\zeta_4 + 3\zeta_6}} \operatorname{csch} \left[\sqrt{-\frac{\zeta_5}{5}} \left(x - v \frac{t^\alpha}{\alpha} \right) \right]}{\pm \sqrt{\sigma_3^2 - 4\sigma_2 \sigma_4} - \sigma_3 \operatorname{csch} \left[\sqrt{-\frac{\zeta_5}{5}} \left(x - v \frac{t^\alpha}{\alpha} \right) \right]} \right\} e^{i(-\kappa x + \omega \frac{t^\alpha}{\alpha} + \vartheta_0)}. \quad (75)$$

Setting $\sigma_3 = 0$ into Eqs. (74) and (75) yields bright and singular solitons:

$$Rq(x, t) = \mp 2 \sqrt{-\frac{3\zeta_5}{2\zeta_4 + 3\zeta_6}} \operatorname{sech} \left[\sqrt{-\frac{\zeta_5}{5}} \left(x - v \frac{t^\alpha}{\alpha} \right) \right] e^{i(-\kappa x + \omega \frac{t^\alpha}{\alpha} + \vartheta_0)}, \quad (76)$$

$$q(x, t) = \pm 2 \sqrt{\frac{3\zeta_5}{2\zeta_4 + 3\zeta_6}} \operatorname{csch} \left[\sqrt{-\frac{\zeta_5}{5}} \left(x - v \frac{t^\alpha}{\alpha} \right) \right] e^{i(-\kappa x + \omega \frac{t^\alpha}{\alpha} + \vartheta_0)}. \quad (77)$$

Finally, straddled solitons are obtained:

$$q(x, t) = \left\{ -\frac{\sigma_2 \sigma_3 \operatorname{sech}^2 \left[\frac{1}{2} \sqrt{-\frac{\zeta_5}{5}} \left(x - v \frac{t^\alpha}{\alpha} \right) \right]}{\sigma_3^2 - \sigma_2 \sigma_4 \left(1 - \tanh \left[\frac{1}{2} \sqrt{-\frac{\zeta_5}{5}} \left(x - v \frac{t^\alpha}{\alpha} \right) \right] \right)^2} \right\} e^{i(-\kappa x + \omega \frac{t^\alpha}{\alpha} + \vartheta_0)}, \quad (78)$$

$$q(x, t) = \left\{ \frac{\sigma_2 \sigma_3 \operatorname{csch}^2 \left[\frac{1}{2} \sqrt{-\frac{\zeta_5}{5}} \left(x - v \frac{t^\alpha}{\alpha} \right) \right]}{\sigma_3^2 - \sigma_2 \sigma_4 \left(1 - \coth \left[\frac{1}{2} \sqrt{-\frac{\zeta_5}{5}} \left(x - v \frac{t^\alpha}{\alpha} \right) \right] \right)^2} \right\} e^{i(-\kappa x + \omega \frac{t^\alpha}{\alpha} + \vartheta_0)}. \quad (79)$$

6. Results and discussion

This section provides a comprehensive analysis of the various soliton solutions presented in Figures 1 through 3. Each figure illustrates the behavior of different soliton types—bright, singular, dark, bright-dark, and singular-singular—under the influence of fractional temporal evolution. The parameters for all figures are set as follows: $a = 1$, $b = 1$, $c_1 = 1$, $c_2 = 1$, $c_3 = 1$, $k = 1$, $\kappa = 1$, $\omega = 1$, $\sigma_2 = 1$, $\delta_{12} = -2$, $\delta_{13} = 1$, $\delta_{14} = 1$, $\delta_1 = -4$, $\delta_2 = 1$, $\delta_3 = 1$, $\delta_4 = \frac{3}{2}$, $\delta_6 = 1$, $\delta_7 = 1$, and $\delta_8 = 1$.

Figure 1 explores the modulus of a bright soliton given by Eq. (50) across fifteen subfigures, displaying its evolution under varying fractional temporal evolution parameter α . The subfigures are divided into surface plots, 2D plots, and contour plots. Figures 1a–c ($\alpha = 0.4$): The bright soliton shows a moderate peak in amplitude with a symmetric profile. The surface plot (1a) captures the soliton's propagation with relatively smooth contours, as confirmed by the contour plot (1b). The 2D plot (1c) reveals a well-defined peak at the soliton's center, with slight broadening due to the lower value of α . Figures 1d–f ($\alpha = 0.6$): As α increases to 0.6, the soliton's peak sharpens, indicating stronger confinement of energy. The surface plot (1d) shows this enhanced peak, and the contour plot (1e) reflects tighter contours around the peak. The 2D plot (1f) demonstrates a sharper central peak with reduced width compared to $\alpha = 0.4$. Figures 1g–i ($\alpha = 0.8$): Further increase in α to 0.8 continues to concentrate the soliton's energy, with the surface plot (1g) depicting a steeper and narrower peak. The contour plot (1h) shows more closely packed contours, and the 2D plot (1i) highlights a significantly sharper peak with minimal broadening. Figures 1j–l ($\alpha = 0.9$): At $\alpha = 0.9$, the bright soliton achieves its highest peak with the narrowest profile, as seen in the surface plot (1j). The contour plot (1k) indicates very tight contours, while the 2D plot (1l) shows an almost delta-like peak, indicating strong localization of the soliton. Figures 1m–o ($\alpha = 1$): With $\alpha = 1$, the soliton reaches its maximum localization and amplitude. The surface plot (1m) displays a highly focused peak, while the contour plot (1n) confirms this with extremely tight contour lines. The 2D plot (1o) exhibits a sharp, narrow peak, nearly resembling a Dirac delta function. Figure 1 demonstrates that increasing α leads to greater localization and higher amplitude of the bright soliton, reflecting the direct influence of fractional temporal evolution on soliton dynamics.

Figure 2 examines the modulus of a dark soliton, as described by Eq. (53). Figures 2a–c ($\alpha = 0.4$): The dark soliton shows a localized dip in amplitude, with the surface plot (2a) illustrating a relatively shallow trough. The contour plot (2b) displays broader, spaced-out contours around the trough, and the 2D plot (2c) shows a smooth dip in amplitude, characteristic of dark solitons. Figures 2d–f ($\alpha = 0.6$): At $\alpha = 0.6$, the trough becomes more pronounced, with the surface plot (2d) indicating a deeper dip. The contour plot (2e) shows tighter contours around the trough, and the 2D plot (2f) reveals a more distinct dip, reflecting increased soliton localization. Figures 2g–i ($\alpha = 0.8$): As α increases to 0.8, the dark soliton's trough becomes deeper and narrower, as shown in the surface plot (2g). The contour plot (2h) demonstrates tighter spacing, while the 2D plot (2i) captures a sharp dip with minimal spreading. Figures 2j–l ($\alpha = 0.9$): With $\alpha = 0.9$, the dark soliton reaches its deepest trough, as seen in the surface plot (2j). The contour plot (2k) features very tight contours around the trough, and the 2D plot (2l) shows a sharp, localized dip, indicating strong soliton confinement. Figures 2m–o ($\alpha = 1$): At $\alpha = 1$, the dark soliton achieves maximum depth and narrowness. The surface plot (2m) shows a deep, sharp trough, while the contour plot (2n) has extremely close contours. The 2D plot (2o) reveals an intense, narrow dip, signifying the strongest localization of the dark soliton. Figure 2 demonstrates that the fractional temporal evolution parameter α significantly affects the depth and localization of dark solitons, with higher values of α resulting in more pronounced and confined dips.

Figure 3 explores the modulus of a bright-dark soliton, combining characteristics of both bright and dark solitons as given by Eq. (69). Figures 3a–c ($\alpha = 0.4$): The bright-dark soliton displays a peak and a dip, with the surface plot (3a) capturing this dual nature. The contour plot (3b) shows concentric rings around the peak and trough, while the 2D plot (3c) reveals a peak followed by a dip, characteristic of bright-dark solitons. Figures 3d–f ($\alpha = 0.6$): Increasing α to 0.6 sharpens both the peak and the dip, with the surface plot (3d) showing a more pronounced contrast. The contour plot (3e) has tighter rings around both features, and the 2D plot (3f) reveals a sharper peak and a deeper dip. Figures 3g–i ($\alpha = 0.8$): At $\alpha = 0.8$, the bright-dark soliton exhibits a highly localized peak and trough. The surface plot (3g) shows the peak and dip closely positioned, with the contour plot (3h) displaying very tight contours. The 2D plot (3i) captures a sharp peak followed by a narrow, deep dip. Figures 3j–l ($\alpha = 0.9$): With $\alpha = 0.9$, the bright-dark soliton's peak and dip

become even more pronounced, as seen in the surface plot (3j). The contour plot (3k) has extremely tight spacing, while the 2D plot (3l) indicates a highly localized peak and a deep dip. Figures 3m-o ($\alpha = 1$): At $\alpha = 1$, the bright-dark soliton reaches maximum localization, with the surface plot (3m) showing a sharp peak and a deep, narrow dip. The contour plot (3n) features closely packed contours, and the 2D plot (3o) reveals a nearly delta-like peak and trough, signifying the strongest confinement. Figure 3 shows that the fractional temporal evolution parameter α affects both the bright and dark components of the bright-dark soliton, with higher α values leading to sharper and more localized peaks and troughs.

The results presented across Figures 1 to 3 clearly indicate that the fractional temporal evolution parameter α plays a critical role in determining the localization, amplitude, and overall dynamics of various soliton types. Higher values of α generally lead to more localized, sharper, and higher amplitude soliton structures, reflecting the sensitivity of soliton behavior to fractional temporal evolution in the studied nonlinear optical systems. These findings contribute to a deeper understanding of soliton dynamics and their potential applications in advanced optical communication systems and other nonlinear wave phenomena.

7. Conclusions

This paper addressed the dispersive concatenation model by the enhanced direct algebraic method to recover the soliton solutions with fractional temporal evolution. The retrieved soliton solutions have emerged through the intermediary Jacobi's elliptic functions which when their respective moduli of ellipticity approached a specific constant. This integration algorithm gave way to additional forms of soliton solutions that were left unclassified. These solitons emerged for special choice and combination of the parameter values. The results are thus quite exhaustive for the model that was considered with Kerr law of SPM. These preliminary results are indeed encouraging for further development to the model. The model is yet to be studied with power-law of SPM and the results of such research activities would be reported with time. Subsequently the model would be later addressed with differential group delay and dispersion-flattened fibers. Such results are on the horizon and are to be soon visible once they are made to connect with the pre-existing one [15–19].

Acknowledgement

One of the authors, AB, is grateful to Grambling State University for the financial support he received as the Endowed Chair of Mathematics. This support is sincerely appreciated.

Conflict of interest

The authors claim that there is no conflict of interest.

References

- [1] Ankiewicz A, Akhmediev N. Higher-order integrable evolution equation and its soliton solutions. *Physics Letters A*. 2014; 378(4): 358-361. Available from: <https://doi.org/10.1016/j.physleta.2013.11.031>.
- [2] Ankiewicz A, Wang Y, Wabnitz S, Akhmediev N. Extended nonlinear Schrödinger equation with higher-order odd and even terms and its rogue wave solutions. *Physical Review E*. 2014; 89: 012907. Available from: <https://doi.org/10.1103/PhysRevE.89.012907>.
- [3] Chowdury A, Kedziora DJ, Ankiewicz A, Akhmediev N. Breather-to-soliton conversions described by the quintic equation of the nonlinear Schrödinger hierarchy. *Physical Review E*. 2015; 91: 032928. Available from: <https://doi.org/10.1103/PhysRevE.91.032928>.

- [4] Chowdury A, Kedziora DJ, Ankiewicz A, Akhmediev N. Soliton solutions of an integrable nonlinear Schrödinger equation with quintic terms. *Physical Review E*. 2014; 91: 032922. Available from: <https://doi.org/10.1103/PhysRevE.90.032922>.
- [5] Chowdury A, Kedziora DJ, Ankiewicz A, Akhmediev N. Breather solutions of the integrable quintic nonlinear Schrödinger equation and their interactions. *Physical Review E*. 2015; 91: 022919. Available from: <https://doi.org/10.1103/PhysRevE.91.022919>.
- [6] Arnous AH, Murad MAS, Biswas A, Yildirim Y, Georgescu PL, Moraru L, et al. Optical solitons for the concatenation model with fractional temporal evolution. *Ain Shams Engineering Journal*. 2025; 16(2): 103243. Available from: <https://doi.org/10.1016/j.asej.2024.103243>.
- [7] Murad MAS, Faridi WA, Iqbal M, Arnous AH, Shah NA, Chung JD. Analysis of Kudryashov's equation with conformable derivative via the modified Sardar sub-equation algorithm. *Results in Physics*. 2024; 60: 107678. Available from: <https://doi.org/10.1016/j.rinp.2024.107678>.
- [8] Murad MAS, Arnous AH, Faridi WA, Iqbal M, Nisar KS, Kumar S. Two distinct algorithms for conformable time- fractional nonlinear Schrödinger equations with Kudryashov's generalized non-local nonlinearity and arbitrary refractive index. *Optical and Quantum Electronics*. 2024; 56: 1320. Available from: <https://doi.org/10.1007/s11082-024-07223-8>.
- [9] Murad MAS, Iqbal M, Arnous AH, Biswas A, Yildirim Y, Alshomrani AS. Optical dromions with fractional temporal evolution by enhanced modified tanh expansion approach. *Journal of Optics*. 2024. Available from: <https://doi.org/10.1007/s12596-024-01979-8>.
- [10] Murad MAS, Arnous AH, Biswas A, Yildirim Y, Alshomrani AS. Suppressing internet bottleneck with Kudryashov's extended version of self-phase modulation and fractional temporal evolution. *Journal of Optics*. 2024. Available from: <https://doi.org/10.1007/s12596-024-01937-4>.
- [11] Ekici M, Sarmasik CA. Certain analytical solutions of the concatenation model with a multiplicative white noise in optical fibers. *Nonlinear Dynamics*. 2024; 112: 9459-9476. Available from: <https://doi.org/10.1007/s11071-024-09478-y>.
- [12] Ekici M, Sarmasik CA. Various dynamic behaviors for the concatenation model in birefringent fibers. *Optical and Quantum Electronics*. 2024; 56: 1342. Available from: <https://doi.org/10.1007/s11082-024-07252-3>.
- [13] Akram U, Tang Z, Althobaiti S, Althobaiti A. Dynamics of optical dromions in concatenation model. *Nonlinear Dynamics*. 2024; 112: 14321-14341. Available from: <https://doi.org/10.1007/s11071-024-09810-6>.
- [14] Khan MAU, Akram G, Sadaf M. Dynamics of novel exact soliton solutions of concatenation model using effective techniques. *Optical and Quantum Electronics*. 2024; 56: 385. Available from: <https://doi.org/10.1007/s11082-023-05957-5>.
- [15] Wang TY, Zhou Q, Liu WJ. Soliton fusion and fission for the high-order coupled nonlinear Schrödinger system in fiber lasers. *Chinese Physics B*. 2022; 31(2): 020501. 10.1088/1674-1056/ac2d22
- [16] Liang YH, Wang KJ. Bifurcation analysis, chaotic phenomena, variational principle, Hamiltonian, solitary and periodic wave solutions of the fractional Benjamin Ono equation. *Fractals*. 2025; 33(01): 1-13. Available from: <https://doi.org/10.1142/S0218348X25500161>.
- [17] Wang KJ, Liu JH, Si J, Shi F, Wang GD. N -soliton, breather, lump solutions and diverse traveling wave solutions of the fractional $(2 + 1)$ -dimensional Boussinesq equation. *Fractals*. 2023; 31(03): 2350023. Available from: <https://doi.org/10.1142/S0218348X23500238>.
- [18] Wang KJ. On the generalized variational principle of the fractal Gardner equation. *Fractals*. 2023; 31(09): 2350120. Available from: <https://doi.org/10.1142/S0218348X23501207>.
- [19] Wang KJ, Wang GD, Shi F, Liu XL, Zhu HW. Variational principle, Hamiltonian, bifurcation analysis, chaotic behaviors and the diverse solitary wave solutions of the simplified modified Camassa-Holm equation. *International Journal of Geometric Methods in Modern Physics*. 2025; 25500136. Available from: <https://doi.org/10.1142/S0219887825500136>.